ELSEVIER

Catalysis Today 57 (2000) 275–282

CATALYSIS TODAY

www.elsevier.com/locate/cattod

The promoting effect of Nb_2O_5 addition to Pd/Al_2O_3 catalysts on propane oxidation

F.B. Noronha[1], D.A.G. Aranda[2], A.P. Ordine, Martin Schmal *

NUCAT-PEQ-COPPE, Universidade Federal do Rio de Janeiro, Ilha do Fundão, COPPE, CP 68502, CEP 21941, Rio de Janeiro, Brazil

Abstract

$Pd/Nb_2O_5/Al_2O_3$ catalysts were investigated on propane oxidation. Diffuse reflectance spectroscopy (DRS) and X-ray photoelectron spectroscopy (XPS) analysis suggested that monolayer coverage was attained between 10 and 20 wt.% of Nb_2O_5. Temperature programmed reduction (TPR) evidenced the partial reduction of niobium oxide. The maximum propane conversion observed on the Pd/10% Nb_2O_5/Al_2O_3 corresponded to the maximum Nb/Al surface ratio. The presence of NbO_x polymeric structures near to the monolayer could favor the ideal Pd^0/Pd^{2+} surface ratio to the propane oxidation which could explain the promoting effect of niobium oxide.

Keywords: Propane oxidation; Niobium oxide; Calcination

1. Introduction

There has been great interest in studying the promoting effects of oxides on supported metal catalysts [1–3]. The metal–oxide interaction induces important modifications of the adsorption and catalytic properties of the metal in several reactions.

It has been reported the presence of a strong metal–support interaction (SMSI) in supported metal-oxide catalysts [1–3]. Hu et al. [1] studied the extent of $Rh–Nb_2O_5$ interaction in the niobia-promoted Rh/SiO_2 catalysts. The NbO_2 species formed during the reduction at high temperature blocks the surface of Rh atoms and may cause the decrease of both the H_2 chemisorption capacity and the activity of ethane hydrogenolysis. In contrast to these catalysts, Nb_2O_5 monolayers on SiO_2 promoted Pt catalysts without suppression by SMSI [3]. The higher selectivity of the lanthana promoted Pd/SiO_2 catalysts towards methanol synthesis on CO hydrogenation was attributed to the decoration of the Pd particles by partially reduced LaO_x moieties [3]. According to Rieck and Bell [3], these LaO_x species promote the dissociation of adsorbed CO, which favor the methanol synthesis.

Alumina-supported Pd-based metal oxides have received increasing attention in recent years, mainly due to their use in automotive emissions control. Ceria has been used mainly as an oxygen storage component [4,5]. The ceria addition promotes the CO oxidation as well as the NO reduction through a bifunctional mechanism based on the redox properties of the reducible support [5,6]. The addition of MoO_3 to Pd/Al_2O_3 improved the NO conversion with very

* Corresponding author. Fax: +55-21-2906626.
E-mail addresses: bellot@peq.coppe.ufrj.br (F.B. Noronha), donato@h2o.eq.ufrj.br (D.A.G. Aranda), schmal@peq.coppe.ufrj.br (M. Schmal).
[1] Present address: Instituto Nacional de Tecnologia (INT), Av. Venezuela 82, CEP 20081-310, Rio de Janeiro, Brazil. Fax: +55-21-2636552.
[2] Present address: Escola de Química, Universidade Federal do Rio de Janeiro, Ilha do Fundão, CP 68542, Rio de Janeiro, Brazil. Fax: +55-21-5904991.

0920-5861/00/$ – see front matter
PII: S0920-5861(99)00337-5

low NH_3 formation even in the presence of a small excess of oxygen [7–9]. This catalytic behavior has been explained by a strong interaction between the noble metal and the partially reduced molybdenum oxide.

In spite of its redox properties, there are only few studies concerning the use of the niobium oxides as a promoter of Pd/Al_2O_3 catalysts on the CO/NO/HC reaction. Rasband and Hecker [10] performed the NO reduction on $Rh–Nb_2O_5/SiO_2$ catalysts. The addition of Nb_2O_5 to Rh/SiO_2 catalysts diminished the reaction rate, which was ascribed to a decrease of the Rh dispersion. However, it was not presented the selectivity behavior of these catalysts.

The aim of this work was to study the $Pd/Nb_2O_5/Al_2O_3$ systems as a potential catalyst for the oxidation of propane. In this paper, these systems will be characterized through diffuse reflectance spectroscopy (DRS), temperature programmed reduction (TPR) and X-ray photoelectron spectroscopy (XPS) in order to better understand the nature and the extent of $Pd–Nb_2O_5$ interaction and the redox properties. Evidences of promotion on propane oxidation over reduced niobia-based catalysts will be discussed.

2. Experimental

2.1. Catalyst preparation

Al_2O_3 (Degussa) and Nb_2O_5 were used as supports. Al_2O_3 was calcined in air at 823 K for 16 h (BET area=180 m^2/g). Nb_2O_5 was prepared by calcination of niobic acid CBMM (Companhia Brasileira de Metalurgia e Mineração) as described for alumina.

Nb_2O_5/Al_2O_3 samples were prepared by Al_2O_3 impregnation with an aqueous solution of niobium oxalate CBMM in oxalic acid at pH=0.5 [11]. The samples were dried at 373 K under vacuum and calcined under air flow at 823 K for 16 h.

Pd/Al_2O_3, Pd/Nb_2O_5 and $Pd/Nb_2O_5/Al_2O_3$ samples were obtained by incipient-wetness impregnation of Al_2O_3, Nb_2O_5 and Nb_2O_5/Al_2O_3, respectively, with a hydrochloric acid solution of $PdCl_2$. Then, the samples were dried at 373 K for 16 h followed by calcination under air flow at 773 K for 2 h.

The prepared catalysts and their metal contents measured by atomic absorption are given in Table 1.

Table 1
Catalyst composition and palladium dispersion obtained through hydrogen chemisorption

Sample	Pd (wt.%)	Nb_2O_5 (wt.%)	Dispersion (%)
Pd/Al_2O_3	1.25	–	36
Pd/1% Nb_2O_5/Al_2O_3	1.03	0.98	37
Pd/5% Nb_2O_5/Al_2O_3	0.91	5.66	28
Pd/10% Nb_2O_5/Al_2O_3	1.10	9.10	15
Pd/20% Nb_2O_5/Al_2O_3	0.94	21.90	7
Pd/Nb_2O_5	0.97	–	5

2.2. Diffuse reflectance spectroscopy

The diffuse reflectance spectra were recorded between 200 and 900 nm on an UV–Vis NIR spectrometer (Cary 5 — Varian) equipped with an integrating sphere (Harrick). In the case of Pd/Al_2O_3 and Pd/Nb_2O_5 samples, Al_2O_3 and Nb_2O_5 were used as references, respectively. For Pd/*x*% Nb_2O_5/Al_2O_3 (*x*%=1, 5, 10 and 20 wt.%), the corresponding references of *x*% Nb_2O_5/Al_2O_3 samples were used.

2.3. Temperature programmed reduction

TPR experiments were performed in a conventional apparatus, as described previously [12]. Before reduction, the catalysts were heated at 423 K in flowing argon for 0.5 h. Then, a mixture of 1.6% hydrogen in argon flow was passed through the sample and the temperature was raised from 298 up to 1173 K at a heating rate of 10 K/min.

2.4. X-ray photoelectron spectroscopy

XPS was performed in a Perkin-Elmer 1257 spectrometer by using a Mg Kα (1253.6 eV) radiation and operating at 15 kV/200 W. The photoelectron's kinetic energy was measured by a hemispheric analyzer, with a 46.95 eV/step passage energy. The vacuum in the spectrometer chamber was 10^{-9} Torr, and the charge correction was obtained by using the Al (2p) emission at 74.0 eV line as reference. The Nb/Al surface ratios of the niobium oxide on the alumina support were calculated from photoelectron peak areas of the Nb (3d) and Al (2p) photoelectron lineshapes after correction of the photoionization cross-sections and photoelectron mean free paths [13]. The samples were analyzed

in the oxide form after calcination (C). In order to evaluate the presence of chloride ions, Pd/Al_2O_3 and Pd/20% Nb_2O_5/Al_2O_3 were also analyzed after reduction (R). Hydrogen treatment of the sample was carried out in a reaction chamber at 773 K for 2 h (10 K/min). After reduction, the sample was cooled and evacuated before inserting into the spectrometer without exposure to air.

2.5. H_2 chemisorption

The chemisorption uptakes were measured in an ASAP (Micrometrics) apparatus. Before the reduction, the catalysts were dehydrated at 423 K for 0.5 h. Then the catalysts were reduced at 773 K (5 K/min) in flowing H_2 (30 cm^3/min). Following reduction, the samples were evacuated for 1 h at reduction temperature and cooled to adsorption temperature under vacuum. Irreversible uptakes were determined from dual isotherms measured for hydrogen (at 343 K) using the method of Benson et al. [14].

2.6. Propane oxidation

The oxidation of propane was performed in a flow microreactor at atmospheric pressure. The catalyst (ca. 50 mg) was mixed with quartz as diluent (500 mg), dried with flowing nitrogen at 393 K, and then reduced with hydrogen at 773 K for 2 h. After reduction, the reaction was carried out from 473 to 773 K in intervals of 20 K. The reaction mixture consisted of 2% O_2/0.4% C_3H_8/97.6% N_2 (flow rate=200 ml/min). Analyses were obtained by on line gas chromatography (FID) with a Haysep D column (6 m, carrier gas: H_2). Thus, propane conversions were calculated from the molar balance.

3. Results

The DRS spectra of Pd/Al_2O_3, Pd/Nb_2O_5 and $Pd/Nb_2O_5/Al_2O_3$ are presented in Fig. 1. The spectrum of the Pd/Al_2O_3 sample exhibits 3 bands at 287, 325 and 458 nm (Table 2). According to the literature, the band at 287 nm is ascribed to metal–ligand charge transfer [15]. The band located around 325 nm arises from $Pd(H_2O)_4^{2+}$ complex since the measurements were performed in contact with air. The band at 458 nm is attributed to a d–d transition. On the other hand, the spectrum of Pd/Nb_2O_5 sample shows only the ν_3 band displaced to 407 nm.

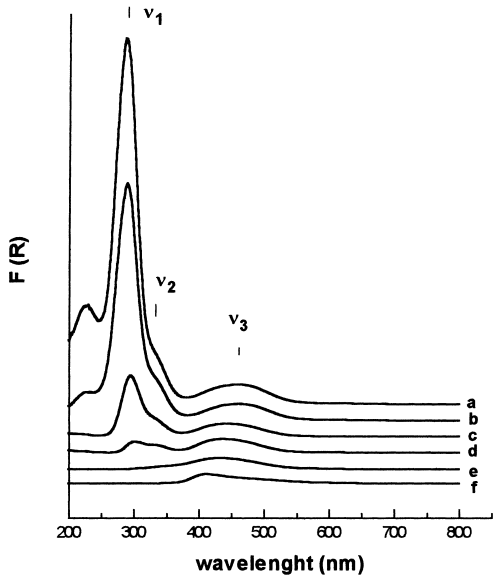

Fig. 1. DRS spectra of (a) Pd/Al_2O_3; (b) Pd/1% Nb_2O_5/Al_2O_3; (c) Pd/5% Nb_2O_5/Al_2O_3; (d) Pd/10% Nb_2O_5/Al_2O_3; (e) Pd/20% Nb_2O_5/Al_2O_3; (f) Pd/Nb_2O_5.

The addition of Nb_2O_5 modified significantly the spectra of the Pd/Al_2O_3 sample. Increasing the Nb_2O_5 content, the intensity of the charge transfer band decreased and this band was shifted towards higher wavelengths. When the niobium oxide loading is 20 wt.%, the ν_1 band is no more observed.

Table 2
Position of UV–Vis bands observed on Pd/Al_2O_3, Pd/Nb_2O_5 and $Pd/Nb_2O_5/Al_2O_3$ samples

Sample	λ (nm)		
	ν_1[a]	ν_2[b]	ν_3[b]
Pd/Al_2O_3	287	325	458
Pd/1% Nb_2O_5/Al_2O_3	289	327	455
Pd/5% Nb_2O_5/Al_2O_3	294	332	445
Pd/10% Nb_2O_5/Al_2O_3	302	340	437
Pd/20% Nb_2O_5/Al_2O_3	–	–	432
Pd/Nb_2O_5	–	–	407

[a] Metal to ligand charge transfer (spin allowed) [1].
[b] d–d transition (spin allowed) [1].

Table 3
Binding energies and intensity ratios for the XPS spectra of the $Pd/Nb_2O_5/Al_2O_3$ samples

Catalyst	Binding energy (eV)			Ratios	
	Pd ($3d_{5/2}$)	Nb ($3d_{5/2}$)	O (1s)	I_{Nb}/I_{Al}	$(Nb/Al)_s$[a]
Pd/1% Nb_2O_5/Al_2O_3	336.0	206.6	530.8	0.5375	0.0431
Pd/5% Nb_2O_5/Al_2O_3	335.9	206.7	530.7	1.8565	0.1487
Pd/10% Nb_2O_5/Al_2O_3	336.0	206.7	530.6	3.1249	0.2503
Pd/20% Nb_2O_5/Al_2O_3	336.1	206.9	530.7	2.2471	0.1800

[a] Surface atomic ratio calculated from the integrated areas of the Nb (3d) and Al (2p) photoelectron lines.

Table 3 presents the binding energies and the intensity ratios of the main elements in the $Pd/Nb_2O_5/Al_2O_3$ catalysts. The increase of the niobium content does not change the binding energy values of the Pd ($3d_{5/2}$), Nb ($3d_{5/2}$) and O (1s) lines. However, the intensity ratios and the Nb/Al surface ratio exhibited a maximum around 10 wt.% of Nb_2O_5 (Fig. 2). The Cl/Al and Cl/Nb atomic ratios before and after the reduction of the Pd/Al_2O_3 and $Pd/Nb_2O_5/Al_2O_3$ catalysts are shown in Table 4. The reduction at 773 K led to a strong diminution of the Cl/Al and Cl/Nb atomic ratio on both catalysts.

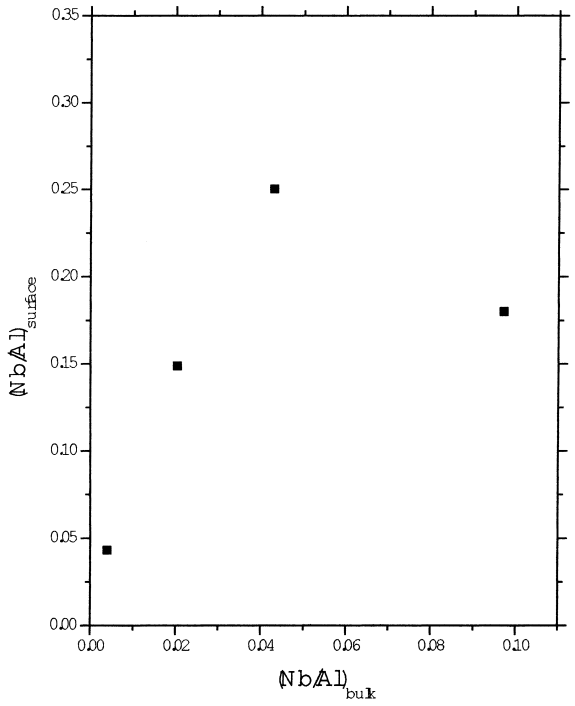

Fig. 2. XPS intensity ratios of (Nb/Al) surface as a function of (Nb/Al) bulk.

The TPR profiles of Pd/Al_2O_3, Pd/Nb_2O_5 and $Pd–Nb_2O_5/Al_2O_3$ are shown in Fig. 3. The Pd/Al_2O_3 catalyst shows one peak at 429 K and a broad desorption peak at high temperature. On the other hand, the TPR profile of the Pd/Nb_2O_5 catalyst is completely different. In this case, a hydrogen consumption is observed at room temperature followed by a negative peak around 380 K. At high reduction temperature, it shows two peaks at 516 and 1195 K.

The Pd/1% Nb_2O_5/Al_2O_3 catalyst exhibits a peak at 427 K and a small hydrogen uptake above 1100 K. As the Nb_2O_5 content is increased the peak around 429 K is displaced to lower temperatures and a hydrogen consumption appeared between 560 and 930 K. The Pd/20% Nb_2O_5/Al_2O_3 catalyst displays three reduction peaks at 410, 676 and 1060 K.

The results of palladium dispersion calculated from H_2 chemisorption are listed in Table 1. In relation to Pd/Al_2O_3 catalyst, the presence of 1% Nb_2O_5 do not practically modify the palladium dispersion value. On the other hand, the addition of more niobium oxide decreased continuously the hydrogen adsorption capacity.

Fig. 4 presents the conversion of propane as a function of the reaction temperature on $Pd/Nb_2O_5/Al_2O_3$

Table 4
Cl/Al and Cl/Nb atomic ratios of the Pd/Al_2O_3 and Pd/20% Nb_2O_5/Al_2O_3 after calcination (C) and reduction (R)

Catalysts	Cl/Al	Cl/Nb
Pd/Al_2O_3 (C)	0.03	–
Pd/Al_2O_3 (R)	0.007	–
Pd/20% Nb_2O_5/Al_2O_3 (C)	0.12	0.79
Pd/20% Nb_2O_5/Al_2O_3 (R)	0.005	0.02

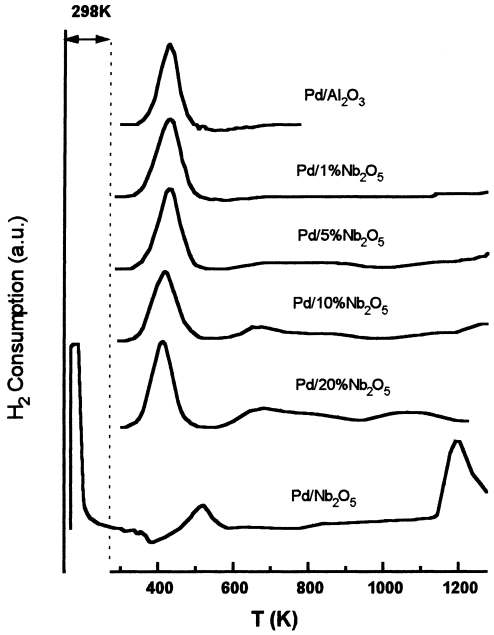

Fig. 3. TPR profile of $Pd/Nb_2O_5/Al_2O_3$ catalysts.

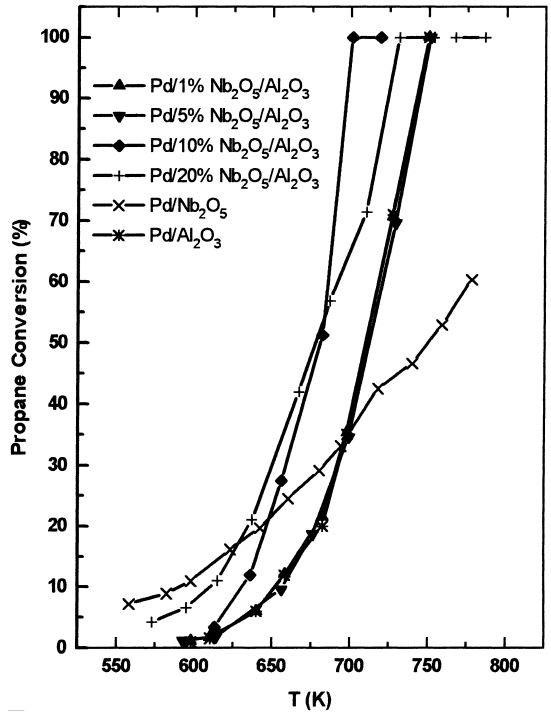

Fig. 4. Conversion of propane as a function of the reaction temperature on $Pd/Nb_2O_5/Al_2O_3$ catalyst.

catalysts. As shown, the niobia addition promotes the propane oxidation at lower temperatures than standard Pd/Al_2O_3 catalyst. The Pd/10% Nb_2O_5/Al_2O_3 is the most active catalyst. However, Pd/Nb_2O_5 catalyst presented low activity with a maximum propane conversion of 60% at 773 K.

4. Discussion

The Pd environment on Pd/Al_2O_3 has been studied by UV–Vis diffuse reflectance spectroscopy after calcination with oxygen at different temperatures [15]. In the case of the catalyst prepared from $PdCl_2$ precursor, the increase of the calcination temperature reduced the absorbance of the charge transfer band at 280 nm and displaced the ν_3 band from 475 to 450 nm. According to the authors, these results indicate that chloride ions were partially removed from the Pd^{2+} coordination sphere at high calcination temperature. Thus, the Pd^{2+} ions would be linked to surface oxygen atoms of alumina or would form small PdO particles. Furthermore, the spectrum of the Pd/Al_2O_3 sample prepared from nitrate precursor showed a broad peak around 380 nm which was attributed to supported PdO.

Lomot et al. [16] used UV–Vis diffuse reflectance spectroscopy to study the effect of calcination conditions on the structure of Pd/SiO_2 catalysts prepared from $PdCl_2$. The UV–Vis spectra showed two bands at 370 and 510 nm. The first one was attributed to $Pd(H_2O)_4^{2+}$ species. The latter one was shifted to 476 nm as the calcination temperature was increased. According to them, the shift was due to the incorporation of oxygen into coordination sphere of Pd replacing chloride ions.

The intensity of the ν_1 band decreases as the Nb_2O_5 loading increases suggesting that less chloride ions are present on the Pd^{2+} coordination sphere (Table 2). It is important to stress that Pd/Nb_2O_5 samples did not retain chloride ions since only the band around 400 nm was identified on this catalyst which can be attributed to supported PdO species. It means that as palladium is deposited over niobium oxide, the characteristic band of charge transfer is not observed. Therefore, the DRS analysis could be used as a tool for determination of monolayer coverage formation on $Pd/Nb_2O_5/Al_2O_3$ samples. The DRS spectra suggests that the monolayer coverage occurs between 10 and

20 wt.% of Nb_2O_5 since the ν_1 band was not observed in the 20% Nb_2O_5/Al_2O_3 sample. In addition, the XPS results showed a maximum around 10 wt.% Nb_2O_5 in the curve of $(Nb/Al)_s$ vs $(Nb/Al)_b$ (Fig. 2) which confirms that the monolayer was reached. These results agree very well with the XPS and Raman studies of Nb_2O_5/Al_2O_3 systems [11,17]. It was found that above 19% Nb_2O_5/Al_2O_3, the monolayer coverage was exceeded and Nb_2O_5 particles were present.

Rakai et al. [15] also compared the diffuse reflectance spectra of pure PdO with those of alumina supported Pd samples prepared from chloride and nitrate precursors. According to them, the shift of the wavelength of the band in the d–d transition region stems from the particle size of palladium. The band at 380 nm was attributed to large particles produced after calcination of $Pd(NO_3)_2$ precursor whereas the band at 450 nm was due to smaller ones produced from $PdCl_2$ precursor.

Lomot et al. [16] observed that the incorporation of oxygen into Pd–Cl complexes seems to favor the metal dispersion. The calcination at temperatures above 773 K favors a great removal of chlorine and the formation of large PdO particles.

Fig. 1 shows that the band at 436 nm on Pd/Al_2O_3 shift towards 410 nm on Pd/Nb_2O_5. As proposed by Rakai et al. [15], this result suggests that the Pd/Al_2O_3 exhibits higher dispersion than the Pd/Nb_2O_5. The Pd oxychloride species present on Pd/Al_2O_3 would be more strongly attached to the support surface producing high metal dispersions. On the other hand, low dispersion is expected on Pd/Nb_2O_5 sample since the PdO was the main species. These results agree well with the dispersion calculated from hydrogen adsorption (Table 1).

TPR results confirm the DRS analysis. Since the Pd oxychloride species are stronger linked to the support than the PdO species their reduction will occur at higher temperatures. The TPR profiles of Pd/Al_2O_3 and Pd/Nb_2O_5 catalysts support this statement. Then, the peak at 429 K is attributed to PdO_xCl_y reduction whereas the hydrogen uptake at room temperature corresponds to PdO reduction. In addition to the reduction of PdO, hydrogen absorption in the reduced palladium and adsorption at the metallic surface are also responsible for the hydrogen consumption at room temperature [12,18,19]. The negative peak is generally attributed to the desorption of weakly adsorbed hydrogen from the palladium surface and the decomposition of palladium hydride formed at room temperature [12,18,19].

On the $Pd/Nb_2O_5/Al_2O_3$ catalysts, the niobium oxide addition shifted the peak ascribed to PdO_xCl_y reduction from 429 K (Pd/Al_2O_3) to 410 K (Pd/20% Nb_2O_5/Al_2O_3). According to DRS results, the increase of Nb_2O_5 loading enhances the incorporation of oxygen into coordination sphere of Pd replacing gradually the chloride ligands. Furthermore, the hydrogen consumption at high temperature corresponds to the niobium oxide reduction. Hu et al. [1] characterized $Rh/Nb_2O_5/SiO_2$ catalysts by TPR. They also attributed the hydrogen uptake at high temperature to the partial reduction of the niobia.

4.1. The promoting effect of Nb_2O_5 addition

Recently, the mechanism of light hydrocarbons oxidation on noble metals has received significant attention, searching to describe this very specific type of reaction.

In fact, a lot of parameters can promote or inhibit the oxidation of molecules like methane or propane. Particle size [20–22] and different amounts of water, CO_2 and chlorine [23,24] are some of the variables which can modify the catalytic activity. On palladium based catalysts, even the nature of active phase has been discussed in literature. A redox model involving a skin of PdO on Pd^0 particles [25–27] as the active phase which promote the oxidation of hydrocarbons is the most acceptable model. In addition, Muto et al. [28,29] showed the importance of the nature of the support which needs to be resistant to sintering and weakly interact with the loaded metal or metal oxide. It has been reported that palladium exhibits the highest activity under weak interaction with the support for $Pd/SiO_2/Al_2O_3$ catalysts.

In our work, the particle size effect can be discarded since the dispersion decreased continuously as the niobia loading increased whereas a maximum in propane conversion was observed at 10 wt.% of niobium oxide.

The promoting effect of niobia addition could also be explained based on the chlorine amount on the samples since UV–Vis indicated differences in the chlorine bonded to palladium on Nb_2O_5/Al_2O_3 catalysts.

XPS measurements were performed to understand the importance of residual amount of chlorine after the reduction of the samples. Table 4 shows the surface atomic ratios from XPS analysis. Surprisingly, the calcined Pd/20% Nb_2O_5/Al_2O_3 presented a larger amount of chlorine at the surface than on Pd/Al_2O_3 catalyst. According to the UV–Vis data the chlorine cannot be bonded to palladium, the active phase, and thus it is probably dispersed over the support of the Nb_2O_5/Al_2O_3 catalysts. Noteworthy is that after reduction the total amount of chlorine at the surface decreased strongly and is very small on both samples. Thus, these results suggest that chlorine does not affect significantly the propane oxidation on the $Pd/Nb_2O_5/Al_2O_3$ catalysts.

The better performance of the Pd/10% Nb_2O_5/Al_2O_3 and Pd/20% Nb_2O_5/Al_2O_3 catalysts could be related to the presence of NbO_x species in intimate contact with palladium on niobia loading near to the monolayer. In fact, infrared spectroscopy of adsorbed CO on Pd/Al_2O_3 and $Pd/Nb_2O_5/Al_2O_3$ catalysts after propane oxidation showed that the amount of Pd^0 and Pd^{2+} species was function of Nb_2O_5 loading [27]. It was observed that the partially reduced niobia species prevented the palladium oxidation. According to Garbowiski et al. [26], a redox process involving surface Pd^0 and PdO is a prerequisite for active catalysts. Then, the Pd^0/Pd^{2+} surface ratio could be the determining effect for the catalytic behavior observed.

It is important to stress that DRS and XPS analyses revealed that the monolayer coverage was attained between 10 and 20 wt.% Nb_2O_5. Several niobia species have been found on supported niobium oxide catalysts. Raman studies showed the presence of NbO_4 tetrahedra, slightly and highly distorted NbO_6 octahedra structures on Nb_2O_5/Al_2O_3 systems [11,30,31]. Highly distorted species were present at all loading. At higher surface coverage, polymeric structures were observed. Above 19 wt.% of Nb_2O_5, monolayer coverage was exceeded and bulk Nb_2O_5 was found [31]. XANES and EXAFS analysis revealed three surface species on alumina supported niobium oxide: NbO_4 monomer, Nb_2O_7 dimer and niobic acid like polymer [32]. At low Nb_2O_5 contents, the results suggested the presence of monomer and dimer whereas the niobic acid like compound was the main surface species at high Nb_2O_5 contents. In our work, the DRS and XPS results suggested the presence of bulk Nb_2O_5 species on Pd/20% Nb_2O_5/Al_2O_3 catalyst in agreement with the literature [11,30–32]. Moreover, a straightforward correlation between the conversion results and the $(Nb/Al)_s$ values can be observed. The maximum propane conversion corresponded to the maximum Nb/Al surface ratio indicating that the type of niobium oxide species plays an important role on this reaction. At high niobium content, the appearance of bulk Nb_2O_5 species led to the reduction of propane conversion. Therefore, the presence of NbO_x polymeric structures near to the monolayer could favor the ideal Pd^0/Pd^{2+} surface ratio to the propane oxidation which could explain the promoting effect of niobium oxide.

5. Conclusions

The addition of Nb_2O_5 significantly modified the DRS spectra of the Pd/Al_2O_3 sample. Increasing the Nb_2O_5 content, the intensity of the charge transfer band decreased. When the niobium oxide loading was 20 wt.%, this band was no more observed. These results suggested that chloride ions were partially removed from the Pd^{2+} coordination sphere at high Nb_2O_5 loading. Furthermore, the DRS analysis suggested that the monolayer coverage occurred between 10 and 20 wt.% of Nb_2O_5 since the band of charge transfer was no more observed in the 20% Nb_2O_5/Al_2O_3 sample. In addition, the presence of a maximum around 10 wt.% Nb_2O_5 in the curve of $(Nb/Al)_s$ vs $(Nb/Al)_b$ confirmed that the monolayer was attained around this point. The TPR profile of $Pd/Nb_2O_5/Al_2O_3$ catalyst revealed the partial reduction of niobium oxide. The presence of NbO_x polymeric structures near to the monolayer could favor the ideal Pd^0/Pd^{2+} surface ratio to the propane oxidation which could explain the promoting effect of niobium oxide.

References

[1] Z. Hu, K. Kunimori, T. Uchijima, Appl. Catal. 69 (1991) 253.
[2] Z. Hu, H. Nakamura, K. Kunimori, H. Asano, T. Uchijima, J. Catal. 112 (1988) 478.
[3] J.S. Rieck, A.T. Bell, J. Catal. 96 (1985) 88.
[4] K.C. Taylor, Catal. Rev. Sci. Eng. 35 (1993) 457.
[5] H. Cordatos, R.J. Gorte, J. Catal. 159 (1996) 112.
[6] H. Praliaud, A. Lemaire, J. Massardier, M. Prigent, G. Mabilon, in: J.W. Hightower, W.N. Delgass, E. Iglesia, A.T.

Bell (Eds.), Studies in Surface Science and Catalysis, Vol. 101, Proceedings of 11th International Congress on Catalysis, Elsevier, Amsterdam, 1996, p. 345.
[7] K.M. Adams, H.S. Gandhi, Ind. Eng. Chem. Prod. Res. Dev. 22 (1983) 207.
[8] H.S. Ghandi, H.C. Yao, H.K. Stepien, in: A.T. Bell, L.L. Hegedus (Eds.), Catalysis Under Transient Conditions, ACS Symposium Series No. 178, American Chemical Society, Washington, DC, 1982, p. 143.
[9] I. Halasz, A. Brenner, M. Shelef, Appl. Catal. B 2 (1993) 131.
[10] P.B. Rasband, W.C. Hecker, Catal. Today 8 (1990) 99.
[11] J.M. Jehng, I.E. Wachs, Proceedings of Symposium on New Materials, and Techniques, Miami, Vol. 34, 1989, American Chemical Society, Washington, DC, p. 546.
[12] F.B. Noronha, M. Primet, R. Frety, M. Schmal, Appl. Catal. 78 (1991) 125.
[13] J.H. Scofield, J. Elect. Spectrosc. Relat. Phenom. 8 (1976) 129.
[14] J.E. Benson, H.S. Hwang, M. Boudart, J. Catal. 30 (1973) 146.
[15] A. Rakai, D. Tessier, F. Bozon-Verduraz, New J. Chem. 16 (1992) 869.
[16] D. Lomot, W. Juszczyk, J. Pielaszek, Z. Kaszkur, T.N. Bakuleva, Z. Karpinski, New J. Chem. 19 (1995) 263.
[17] M.A. Vuurman, I.E. Wachs, J. Phys. Chem. 96 (1992) 5008.
[18] G. Chen, W.T. Chou, C.T. Yeh, Appl. Catal. 8 (1983) 389.
[19] T.C. Chang, J.J. Chen, C.T. Yeh, J. Catal. 96 (1985) 51.
[20] T.R. Baldwin, R. Burch, Appl. Catal. 66 (1990) 337.
[21] T.R. Baldwin, R. Burch, Appl. Catal. 66 (1990) 359.
[22] N.M. Rodriguez, S.G. Oh, R.A. Dalla-Beta, R.T.K. Baker, in: B. Delmon, G.F. Froment (Eds.), Catalyst Deactivation, Elsevier, Amsterdam, 1994, p. 417.
[23] F.H. Ribeiro, M. Chow, R.A. Dalla-Beta, J. Catal. 146 (1994) 537.
[24] D.O. Simone, T. Kennelly, N.I. Brungard, R.J. Farrauto, Appl. Catal. 70 (1991) 87.
[25] R. Burch, Catal. Today 35 (1997) 27.
[26] E. Garbowiski, M. Primet, Appl. Catal. 125 (1995) 185.
[27] D.A.G. Aranda, A.P. Ordine, F.B. Noronha, M. Schmal, Phys. Stat. Sol. (a) 173 (1999) 109.
[28] K. Muto, N. Katada, M. Niwa, Catal. Today 35 (1997) 145.
[29] K. Muto, N. Katada, M. Niwa, Appl. Catal. 134 (1996) 203.
[30] J. Jehng, I.E. Wachs, Catal. Today 8 (1990) 37.
[31] M.A. Vuurman, I.E. Wachs, J. Phys. Chem. 96 (1992) 5008.
[32] T. Tanaka, T. Yoshida, H. Yoshida, H. Aritani, T. Funabiki, S. Yoshida, J.M. Jeng, I.E. Wachs, Catal. Today 28 (1996) 71.